Universal Trends Observed in the Maxima of the Longitudinal Velocity Fluctuations and the Zero Crossings in Turbulent Flows

M. A. Badri Narayanan*
Indian Institute of Science, Bangalore, India

I. Introduction

RECENT work by Badri Narayanan et al.[1] has shown that the zero crossings of the velocity fluctuations around the mean have some definite statistical properties. The zero crossing length scale $\Lambda(=U/\pi C)$ where U is the local mean velocity and C is the number of zero crossings per second is found to be log normally distributed with unique mean and standard deviation for grid as well as for boundary-layer flows. The results reported in this Note are a further study on the properties of the turbulent velocity fluctuation based on the concept of zero crossings.

A visual examination of a turbulent velocity trace indicates that the maxima or minima of the fluctuations between zero crossings are exhibited in the form of well-defined peaks which are more pronounced at high Reynolds numbers. Superimposed on these large fluctuations are the small noncrossing ones rich in high frequency contributing substantially to dissipation. When these high-frequency components are removed, the primary large-scale structures emerge and they contain most of the total kinetic energy. In the present investigation, the nonzero crossing fluctuations are neglected and only the primary structures are considered. Further, it is assumed in the data analysis that the duration of the zero crossings T and the maximum amplitude of the velocity fluctuations u'_m between the crossings are the fundamental time and velocity scales. Experiments were conducted on the longitudinal velocity fluctuations in isotropic, free shear, and wall shear flows.

II. Experimental Setup

The experiments were conducted in: 1) two-dimensional zero pressure gradient boundary layers at Reynolds numbers R_θ of 1270, 4550, and 7000 (R_θ based on momentum thickness θ and the freestream velocity U_∞), 2) a two-dimensional jet, and 3) grid flows with different turbulence intensities. A 50.8-cm square low-speed wind tunnel was used for the boundary-layer as well as for the grid experiments. Boundary-layer measurements were made on one of the side walls at a distance of 229 cm downstream of the contraction, where the boundary layer was 3.0-cm thick and fully developed. Mesh sizes of 3.05 cm and 1.27 cm were employed for producing isotropic turbulence. The details of the experimental conditions for the grid as well as for the boundary-layer flows are shown in Tables 1 and 2. A 2.54-cm × 30.48-cm rectangular orifice was used for producing the two-dimensional jet. Air was blown through the orifice at constant pressure. Velocity measurements were made at 24.13 cm downstream of the orifice, where the width of the jet and the center velocity were 11.18 cm and 33.53 m/s, respectively. At this station velocity fluctuations were investigated at four points, namely $y=0$, 1.27, 2.54, and 3.05 cm across the width of the jet, the location $y=0$ corresponding to the center of the flow. A constant temperature hot-wire anemometer was employed for the fluctuating velocities, and the output signals from the anemometer were recorded.

Received Aug. 8, 1978; revision received Jan. 10, 1979.

Index categories: Boundary Layers and Convective Heat Transfer—Turbulent; Jets, Wakes, and Viscid-Inviscid Flow Interactions.

*Professor, Dept. of Aeronautical Engineering.

Table 1 Grid flow parameters

Experiment No.	Mesh size (M), cm	Velocity, m/s	X,[a] cm
1	3.048	7.315	228.6
2	3.048	20.73	228.6
3	3.048	17.68	53.34
4	1.270	18.59	53.34

[a] X is the distance downstream of the grid where measurements were made.

Table 2 Boundary-layer parameters

R_θ	U, m/s	δ, cm
1270	6.09	3.05
4500	12.80	3.05
7000	26.82	3.05

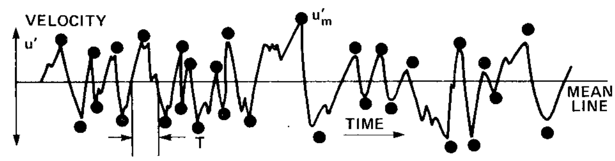

Fig. 1 A typical turbulent velocity trace. (In taking average of u'_m only the magnitude is considered and not the sign.) • = maximum values of u', $\bar{u}'_m$ = average of all u'_m having same T, $\tilde{u}'_m$ = average of all u'_m in a given trace, T = time between two consecutive zero traces.

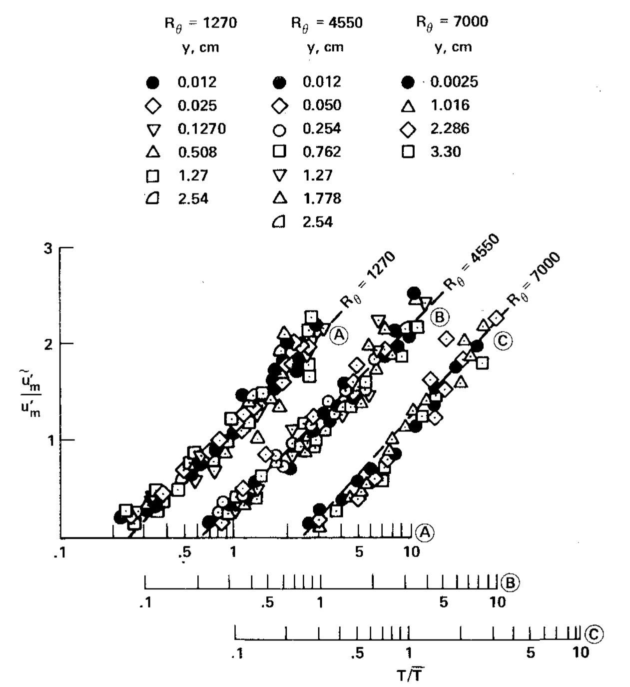

Fig. 2 Relation between u'_m and the duration of the zero crossings in a boundary layer.

III. Experimental Results and Analysis of the Data

The experimental part of the investigation was focused on the determination of the duration T and the peak value of the fluctuations u'_m between two consecutive zero crossings. The signals were rectified around the mean before u'_m was measured. Hence, only the magnitude of u'_m was considered,

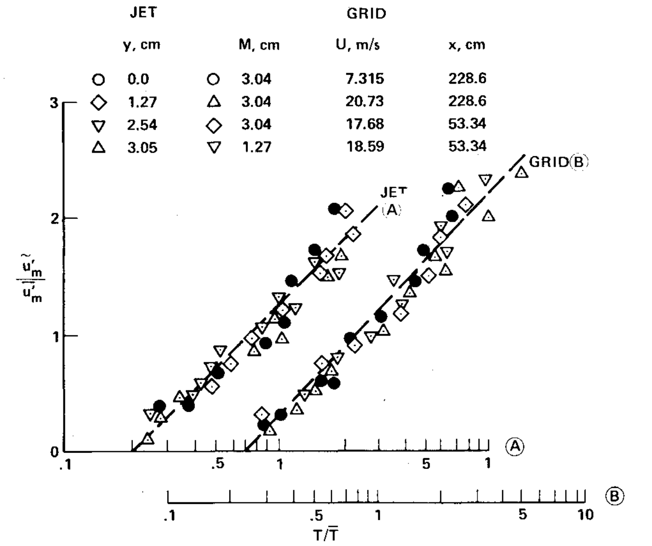

Fig. 3 Relation between u'_m and the duration of the zero crossings in jet and grid flows.

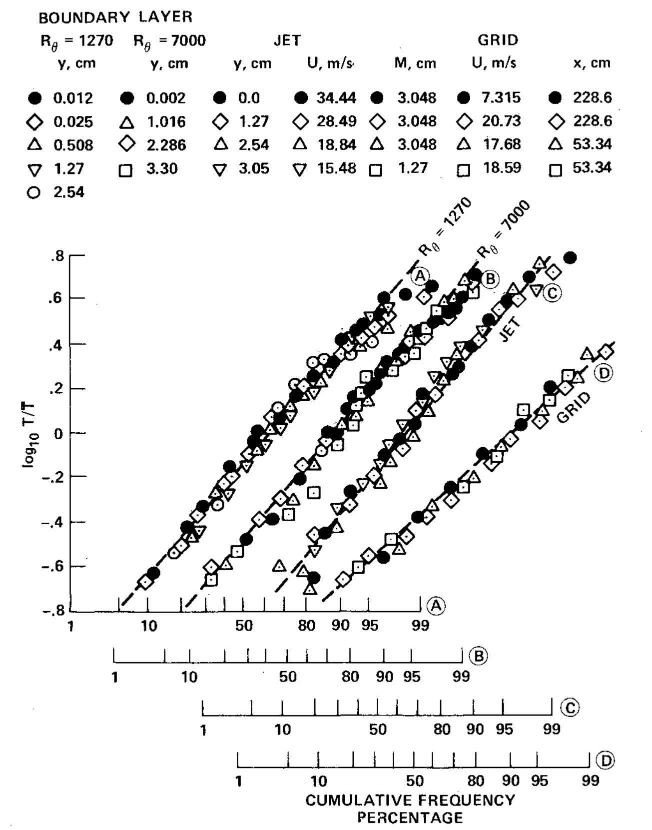

Fig. 4 Probability distribution of T.

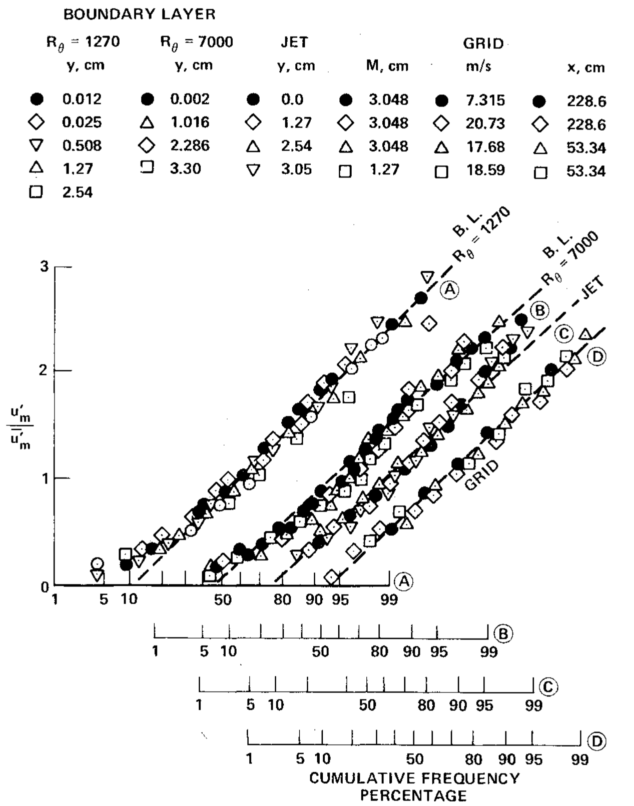

Fig. 5 Probability distribution of u'_m.

not its actual sign. u'_m corresponds to the maximum value of the velocity between two zero crossings (Fig. 1). Here, the arithmetic average of all u'_m in a sample trace is referred to as $\bar{u}'_m$ and, similarly, the average of all values of T as $\bar{T}$. In each experiment a large number of samples, sufficient to warrant a reliable and consistent average, were taken. Since the data were obtained by visual processing in the absence of a computer or an electronic device, a certain amount of scatter could not be avoided. The processing was very time consuming and, as a result, this sample size had to be limited to 1000, which on the average corresponds to a sampling length equal to a flow duration of nearly 2s. The reasonable repeatability of the data within ±5% was a satisfactory indication that the sample size was sufficient to insure the reliability of the results.

Analyses were carried out on the relation between u'_m and T. The values of u'_m were sorted out for a given T from the samples and then averaged. This average is referred to as $\tilde{u}'_m$. In this process, the values of T were discrete and chosen at closer and regular intervals. Any value of u'_m falling within ±10% for a given value of T is considered to belong to that set. When $\tilde{u}'_m$ is normalized with $\bar{u}'_m$ and T with $\bar{T}$, some definite trends could be observed between the two quantities (Figs. 2 and 3). It can be seen that $\tilde{u}'_m$ increases with T. Each point in these figures is obtained from the average of several samples. A large part of the curves seems to follow a straight-line relation when plotted in semilogarithmic form, and the relation seems to be identical in all cases, including the wall region of the boundary layers. At very low values of T, a certain deviation from the straight line exists, but this departure is neglected in the present analysis since u'_m, as well as T in this region, are subjected to certain errors because of the thickness of the recorded trace. The relation between u'_m and T is of the approximate form,

$$\tilde{u}'_m/\bar{u}'_m = C_1 \log_{10}(T/\bar{T} + C_2)$$

where C_1 and C_2 are constants equal to 1.9±0.1 and −0.70, respectively.

The probability distribution of the duration of the zero crossings T, when nondimensionalized with $\bar{T}$, exhibits a near log normal relation for all of the flows. The data are presented in the cumulative frequency percentage form for convenience (Fig. 4). All of the distributions are once again identical, with a standard deviation (σ) of 0.37 and a mean (μ) of about −0.26. σ was estimated as 2/5 of log $(T/\bar{T})$ at 85.5% minus log $(T/\bar{T})$ at 12.5%, and ν as equal to log $(T/\bar{T})$ at 50% of the cumulative frequency percentage. Some difference in σ and μ could be noticed in the case of grid flow measurements. The reason for this could not be traced to experimental errors.

The peak values of u' fluctuations u'_m follow a near-Gaussian distribution for all of the flows studied when $\bar{u}'_m$ is nondimensionalized with $\bar{u}'_m$. The distributions are again identical for all of the flows (Fig. 5) and the values of σ and μ are 0.6 ± 0.05 and 0.09 ± 0.1, respectively. Certain deviations could be observed at low values of u'_m, but this falls within experimental uncertainty. One should remember that in present procedure the mean of u'_m is obtained as an arithmetic average of the modulus of u'_m without taking into consideration the sign of the fluctuations. Thus, the negative and positive parts of the Gaussian distribution in this case are artifically created and do not represent the sign of the signal in the real sense. Only in this way could a single relation be obtained for all of the flows investigated.

The results presented in this Note are somewhat preliminary in nature. Futher investigations are required to understand the significance of these results in relation to the physics of turbulence. The major conclusion of the present work is that the velocity fluctuations in a variety of turbulent flows exhibit some similarity when the duration of the zero crossings and the maximum amplitude of the velocity fluctuations between the corssings are considered as the basic time and velocity scales.

Acknowledgment

The author would like to thank C. S. Subramanian for the help rendered in conducting some of the experiments.

References

[1]Badri Narayanan, M. A., Rajagopalan, S., and Narasimha, R., *Journal of Fluid Mechanics*, Vol. 80, 1977, p. 287.

Peak Strouhal Frequency of Subsonic Jet Noise as a Function of Reynolds Number

Kingo Yamamoto*
State University of New York at Buffalo, Buffalo, N.Y.
and
Roger E. A. Arndt†
University of Minnesota, Minneapolis, Minn.

Introduction

In principle, the sound power of jet noise W is functionally dependent on *both* Reynolds number and Mach number, viz.,

$$W/(\tfrac{1}{2}\rho U^3 D^2) = f(M, R_e)$$

At high Reynolds number, the acoustic power satisfies the approximate relationship

$$W/(\tfrac{1}{2}\rho U^3 D^2) = KM^5$$

where K is a constant. This relationship is confirmed by experiments conducted at moderate to high Reynolds numbers. However, there is some evidence that even at Reynolds numbers of the order of 10^5, the spectral characteristics of jet noise are dependent on Reynolds number, although such evidence has been largely ignored. Mollo-Christensen et al.[1] studied the Reynolds number effects and found that the rms value of the far-field sound pressure is proportional to $(Re)^m$ where m has values of $1 \leq m \leq 3$. Furthermore, they observed that the nondimensional narrow band spectra of the nosie also varied with Reynolds number. Mollo-Christensen[2] conjectured that jet noise will be insensitive to Reynolds number when the boundary layer at the wall is turbulent, which corresponds to Reynolds number of about 2×10^5 based on jet diameter. Above this value of Reynolds number, noise spectra will be similar. Ahuja and Bushall[3] noted that at low Reynolds numbers there is less variation of peak frequency with observation angle. This may be related to the observation by McLaughlin et al.[4] in which the low Reynolds number spectrum was dominated by a few discrete modes.

This Note describes an extension of the previous work. Emphasis is placed on the narrow band spectral characteristics of jet noise. The data reported herein were obtained during an extensive study of the acoustic field generated by subsonic jets at low Reynolds numbers. The results are presented in terms of a dimensionless power spectral density defined by

$$S\left(\frac{fD}{U_j}\right) = \frac{p_f^2/(\rho_0 U_j^2)^2}{D \cdot \Delta f / U_j} \cdot \left(\frac{R}{D}\right)^2$$

where p_f^2 represents the mean square of the pressure fluctuations at frequency f observed in the far field at a distance R.

Experimental Observations

Figures 1 and 2 contain dimensionless spectra plotted as a function of the Strouhal number $Sh = fD/U_j$ for various Reynolds numbers and two Mach numbers. The variation of the sound spectrum with Reynolds number is evident. Three important features should be mentioned. First, the magnitude of the spectrum is an increasing function of the Reynolds number. This is consistent with the observation by Mollo-Christensen et al.[1] Second, the maximum level of the spectrum is not a linear function of Reynolds number. One could conjecture that, at a sufficient low Reynolds number, the flow is completely laminar and no sound is radiated. However, it is questionable whether a jet flow can be completely laminar over all space at any Reynolds number greater than zero. For our purposes this conjecture is probably irrelevant. Third, the spectra are insensitive to Reynolds number above a critical value of about 10^5. The results are inconsistent with the view adopted by Meecham.[5] He argues that the large-scale characteristics of jet turbulence are dependent on the way the jet is generated. Since most of the low-frequency sound is related to the large eddies, the low-frequency end of the sound spectrum will depend upon the driving mechanism of the jet turbulence. On the other hand, he suspects that the high-frequency end of the spectrum may be independent of the driving forces. This view is not supported by the results shown in Figs. 1 and 2. The high-frequency end of the spectra is obviously affected. The sound intensity appears to drop off more rapidly with frequency with the smaller nozzles. Unfortunately, the observed Reynolds number dependence does not follow a simple relationship. It should also be noted that at low Reynolds number, the flow is likely to be very sensitive to the fluctuations of upstream conditions, however small they may be. Thus, the observed acoustic characteristics may vary from one jet to another, even at constant Reynolds number.

One of the most important findings in our jet noise study was that the narrow band peak frequency of the radiated sound is an increasing function of the Reynolds number. It is

Received Oct. 10, 1978; revision received Jan. 16, 1979.

Index categories: Aeroacoustics; Jets, Wakes, and Viscid-Inviscid Flow Interactions.

*Assistant Professor of Research, Dept. of Aerospace Engineering.

†Professor and Director of St. Anthony Falls Hydraulic Laboratory. Member AIAA.